Ultrasonics Sonochemistry 93 (2023) 106298

Contents lists available at ScienceDirect

Ultrasonics Sonochemistry

journal homepage: www.elsevier.com/locate/ultson

Mechanism analysis of hydroxypropyl guar gum degradation in fracture flowback fluid by homogeneous sono-Fenton process

Fuhua Wang [a,1,*], Zezhuang Sun [a,1], Shi Xian[a], Wang Luyi[b], Zhang Weidong[a], Zhang Zhihao[a]

[a] School of Petroleum Engineering, China University of Petroleum, Qingdao, Shandong 266580, China
[b] School of Petroleum and Natural Gas Engineering, Southwest Petroleum University, Chengdu, Sichuan 610500, China

ARTICLE INFO

Keywords:
Sono-Fenton treatment process
Fracture flowback fluid
Hydroxypropyl guar gum
$^{\bullet}$OH radicals

ABSTRACT

An effective hybrid system was applied as the first report for the successful treatment of key pollutants (hydroxypropyl guar gum, HPG) in fracturing flowback fluid, and the synergistic index of the hybrid system was 20.45. In this regard, chemical oxygen demand (*COD*) removal ratio was evaluated with various influencing operating factors including reaction time, H_2O_2 concentration, Fe^{2+} concentration, ultrasonic power, initial pH, and temperature. The optimal operating parameters by single-factor analysis method were: the pH of 3.0, the H_2O_2 concentration of 80 mM, the Fe^{2+} concentration of 5 mM, the ultrasonic power of 180 W, the ultrasonic frequency of 20–25 kHz, the temperature of 39 ℃, the reaction time of 30 min, and the *COD* removal rate reached 81.15 %, which was permissible to discharge surface water sources based on the environmental standards. A possible mechanism for HPG degradation and the generation of reactive species was proposed. Results of quenching tests showed that various impacts of the decomposition rate by addition of scavengers had followed the order of EDTA-2Na < BQ < *t*-BuOH, therefore $^{\bullet}$OH radicals had a dominant role in destructing the HPG. Based on the kinetic study, it was concluded that Chan Kinetic Model was more appropriate to describe the degradation of HPG. Identification of intermediates by GC–MS showed that a wide range of recalcitrant compounds was removed and/or degraded into small molecular compounds effectively after treatment. Under the optimal conditions, the sono-Fenton system was used to treat the fracturing flowback fluid with the initial *COD* value of 675.21 mg/L, and the *COD* value decreased to 80.83 mg/L after 60 min treatment, which was in line with the marine sewage discharge standard. In conclusion, sono-Fenton system can be introduced as a successful advanced treatment process for the efficient remediation of fracture flowback fluid.

1. Introduction

In the past decade, as a mature enhanced oil recovery (EOR)technology, hydraulic fracturing has been widely used in oil and gas exploitation, and over 1 million oil and gas wells have been hydraulically fractured in the United States [1]. However, more and more fracture flowback fluid flows out along with the recovered oil and gas. Shale gas extraction via high volume hydraulic fracturing (HVHF) has resulted in the use of 116 billion liters of fluids annually from 2012 to 2014 and yielded similar volumes of flowback and produced waters [2]. Fracture flowback fluid has a complex composition, which includes dissolved and dispersed organic and inorganic species, microorganisms, and chemical compounds added during drilling and production [3]. Thus, it is generally characterized by high chemical oxygen demand (*COD*), total dissolved solids (*TDS*), stability, and toxicity [4]. According to the investigation, water-based fracturing fluid is the most commonly used fracturing fluid in hydraulic fracturing construction site, while plant gum and its derivatives are the main thickener of water-based fracturing fluid system, accounting for more than 90 %. Since hydroxypropyl guanidine gum contains high non-degradable residue (8–12 %) and water-insoluble matter (20–25 %) [5], hydroxypropyl guanidine gum, as a derivative of plant gum, is the main source of pollutants in fracturing flowback fluid, and the main culprit of environmental harm. The increasing volume of fracture flowback fluid has become a major national concern owing to the rise of induced seismicity in areas of deep-well injection, and the environmental and human health risks associated with the disposal of fracture flowback fluid to unlined impoundments or streams and rivers without adequate treatment [2].

* Corresponding author.
E-mail address: zgsdwfh@126.com (F. Wang).
[1] These authors contributed equally to this work and should be considered co-first authors.

https://doi.org/10.1016/j.ultsonch.2023.106298
Received 18 October 2022; Received in revised form 7 January 2023; Accepted 9 January 2023
Available online 11 January 2023

Meanwhile, environmental protection agency (EPA) states, Constituents commonly found in *TDS* from HF waters may have potential health impacts or create treatment burdens on downstream drinking water systems if discharged at high concentrations to drinking water resources [6]. Therefore, developing treatment technology for removal of the fracture flowback fluid before being discharged to the ecosystem has gained tremendous interest from researchers and has become a hot topic in the environmental protection of oil and gas exploitation.

Today, the commonly used fracturing flowback fluid treatment technologies are mainly physical/ chemical/ biological treatment technologies such as coagulation and flocculation, bag filtration, active carbon adsorption, aeration, chemical precipitation, oil/water separation, membrane filtration [7–13]. These methods are mainly used to remove insoluble solid particles, a small amount of formation crude oil, and organic polymer additives in fracturing fluid components. However, dissolved organic matter is the main component of the flowback fracturing fluid, and the removal effect of the above technologies is poor, far below the sewage discharge standard [14]. In recent years, considerable interest has been shown in the development and application of advanced oxidation processes (AOPs) for the treatment of fracture flowback fluid [3]. AOPs can be defined as an aqueous phase oxidation approach that incorporates in-situ generation of strong oxidizing agents such as peroxydisulfate (PDS, $S_2O_8^{2-}$), peroxymonosulfate (PMS, HSO_5^-), hydroxyl ($^{\bullet}OH$), and sulfate ($SO^{\bullet-}$) that facilitate oxidation of contaminant molecules found in water and wastewater [15–16]. Meanwhile, AOPs are based on the formation of highly reactive species capable of reacting with both organic and inorganic compounds, mineralizing, or at least converting them into less harmful materials [17]. AOPs are garnering increased popularity thanks to their effective and efficient purification of several kinds of contaminants from wastewater, either through their complete mineralization or transformation into less toxic alternatives [15]. Other advantages of AOPs are rapid degradation rates and non-selectivity in the oxidation of contaminants. Some of the individual and hybrid AOPs used for water/wastewater treatment are UV photolysis, photocatalysis, ozonation, sonolysis, Fenton, electro-Fenton, sono-Fenton, sono-photo-Fenton, sonophotocatalytic oxidation, catalytic ozonation, peroxide (O_3/H_2O_2), electrochemical oxidation, persulfate ($S_2O_8^{2-}$), UV/ $S_2O_8^{2-}$, UV/ H_2O_2, hydrodynamic cavitation (HC), HC/O_3, HC/H_2O_2, HC/Fenton, HC/$S_2O_8^{2-}$, HC/photocatalysis, etc. [18–22] Some of these advanced oxidation technologies have been applied to fracturing flowback fluids and have produced good degradation effects [23–25].

Among these treatment technologies, ultrasonic irradiation is considered to be a highly efficient and clean technique without any addition of chemicals and any generation of secondary pollutants [26,27]. The mechanism of ultrasound degradation is based on cavitation, which is the formation, expansion, and sudden collapse of bubbles in liquids. The collapse of these bubbles leads to extremely high local temperatures and pressures (temperatures of roughly 5200 K, pressures of approximately 500 atm) [28–30]. Two possible degradation routes are usually suggested. Firstly, the contaminant can undergo thermal degradation inside the cavity and in the interfacial region (cavity liquid). Secondly, formed free radicals ($^{\bullet}OH$, $^{\bullet}H$, $^{\bullet}O$) can react with the contaminant in the interfacial region or the bulk solution[31]. However, due to the complex chemical properties of wastewater, it is difficult to remove organic matter in the fracturing flowback fluid by ultrasonic cavitation alone. Therefore, it is considered that adding strong oxidants such as hydrogen peroxide, ozone or Fenton reagent in ultrasonic can improve the biodegradability of fracturing flowback fluid [32–34].

The ultrasound based OZONIX reactor has been tested, deployed, and commercialized in all major U.S. unconventional shale plays (Marcellus, Haynesville, Woodford, Fayetteville, Eagle Ford, and Permian Basin), treating more than 76 million barrels (3 + billion gallons) of fluid in a four-year period for various energy exploration and production customers. The combination of ultrasound and ozone is proven to kill bacteria and inhibit scale “on the fly” in various types of completion fluids (flowback, produced, and shallow ground fluids) at very high rates. Operators can use the ultrasound based OZONIX reactor to increase the recycling rate of flowback, produced, and shallow ground fluids and completely eliminate liquid biocides and scale inhibitors from the completions process. The hybrid reactor is mounted on a tractor-trailer unit for portability. Flowback, produced, and/or shallow ground feed waters (in various proportions) are pumped into the hybrid reactor and are flash mixed with introduced ozone. Ultrasonic transducers induce cavitation inside the solution containing dissolved ozone, which results in the shearing of larger particles and a decrease in the particle flotation times. Electrodes present in the hybrid reactor facilitate precipitation of hard salts from the influent [35].

It has been proved that the combination of ultrasound and Fenton agents could significantly remove a wide range of pollutants such as azo dyes [36,37], saline recalcitrant petrochemical wastewater [38], cyanobacterial blooms [39], emerging contaminants [40,41], bisphenol A [42,43] and pharmaceutical wastewater [44,45]. On the one hand, by using ultrasonic irradiation in the reaction medium, the thermal dissociation of water molecules allows the generation of highly reactive $^{\bullet}OH$ radicals and enhances the oxidation power of the Fenton process [46]; on the other hand, Fenton reaction produces a large amount of $^{\bullet}OH$ to promote the removal of organic matter, and the oxygen generated by hydrogen peroxide decomposition can serve as cavitation bubbles to enhance the ultrasonic cavitation effect [45]. Now, the application of sono-Fenton process in fracturing flowbcak fluid is few, and the degradation mechanism of the main pollutants (such as hydroxypropyl guar gum) in the fracturing flowback fluid by sono-Fenton process and the synergistic mechanism of ultrasonic and Fenton technology are rarely reported. Therefore, the study of sono-Fenton degradation mechanism and reaction kinetics of hydroxypropyl guar gum will not only promote the development of sono-Fenton treatment technology for fracturing flowback waste liquid, but also reduce the cost of oilfield fracturing operations and help to achieve the goal of “carbon peak · carbon neutralization” as soon as possible.

In the present study, *COD* removal of HPG by sono-Fenton process was investigated by using hydroxypropyl guar gum as a model pollutant. The main aims of the study are: (a) to investigate the synergy mechanism of sono-Fenton processes by comparing the degradation effects of different treatment technologies (US alone, H_2O_2 alone, $FeSO_4$ alone, US/ $FeSO_4$, US/ H_2O_2, $FeSO_4$/ H_2O_2 and US combined with H_2O_2/ $FeSO_4$) on HPG, (b) to examine the effects of operational parameters including reaction time, H_2O_2 concentration, Fe^{2+} concentration, the ultrasonic power, initial pH and temperature on the degradation efficiency of the HPG, (c) to establish the kinetic equation of the degradation reaction of HPG by sono-Fenton process, (d) to identify the generated intermediates through the HPG degradation by using gas chromatography mass spectrometry (GC–MS), and (e) to analyze the mechanism of the sono-Fenton process in mineralizing HPG.

2. Materials and methods

2.1. Material

Hydroxypropyl guar gum (96.1 %) was purchased from Shanghai Yuanye Biological Technology Co., ltd, China. Hydrogen peroxide (H_2O_2) (30 %), ferrous sulfate ($FeSO_4{\cdot}7H_2O$)(AR), ammonium ferrous sulfate hexahydrate ($Fe(NH_4)_2(SO_4)_2$)(AR), sodium hydroxide (NaOH), sulfuric acid (H_2SO_4) (98 %) were all obtained from Sinopharm Chemical Reagent Co., ltd, China. Potassium titanyl oxalate ($C_4K_2O_9Ti{\cdot}2H_2O$) (AR), hydroxylammonium chloride ($H_3NO{\cdot}HCl$) (99 %) were all obtained from Shanghai Macklin Biochemical Co., ltd, China. 1,10-Phenanthroline (C12H8N2) (99 %), sodium acetate anhydrous (CH_3COONa) (AR), fatty alcohol-polyoxyethylene ether ($RO(CH_2CH_2O)_nH$)(AR), *n*-Butanol ($CH_3(CH_2)_2CH_2OH$)(AR) were all obtained from Shanghai Aladdin Biochemical Technology Co., ltd, China. Citric acid ($C_6H_8O_7$) (AR), triethanolamine ($C_6H_{15}NO_3$)(AR), ammonium persulfate

($(NH_4)_2S_2O_8$)(AR) were all obtained from Laiyang Kangde Chemical Co., ltd, China. YTY-04 organoboron crosslinking agent was obtained from Pucheng Yuteng New Material Technology Co., ltd, China. All the chemicals were of the analytical reagent grade and were used as received from the supplier, without any pretreatment. Distilled water was used to prepare different solutions of required concentrations and was prepared freshly in the laboratory using distillation apparatus.

2.2. Hydration method

In the hydration experiments, hydroxypropyl guar gum solutions with varying concentrations over the range of 0.02 % to 0.1 % (w/w) were prepared based on the detailed methodology described in Amrutlal L's earlier work[47]. The samples (10 mL)were withdrawn, after keeping the prepared polymer solutions overnight in the refrigerator, and measured the initial intrinsic viscosity using an Ubbelohde glass capillary viscometer (Baoying Zhejing glass instrument Factory, China). All the measurements were performed in triplicate and the mean value was taken for the analysis. Comparison of intrinsic viscosity based on different aqueous solutions (0.02 %, 0.05 %, 0.06 %, 0.07 %, 0.1 %) of the hydroxypropyl guar gum showed that concentrations over the range 0.02 % to 0.06 % hydroxypropyl guar gum solutions were appropriate because the ratio of the efflux time of the solution to the efflux time of the solvent is at 1.2 and less than 2.0 to ensure sufficient precision time and reduce the shear effect. Hence 0.06 % of concentration has been selected for the actual study of the effect of different operating parameters.

In the hydration experiments, simulated fracture flowback fluid was prepared based on the detailed methodology described in Lou's earlier work [48]. Firstly, 3.0 g HPG powder was carefully sprinkled into a rapidly swirling vortex of 1000 mL Yelow Sea seawater in a glass beaker obtained using mechanical stirrer. After dissolution, it was left to stand for a period of time so that HPG was completely swollen. Then, 8.0 g anti-swelling cosolvent citric acid, 10 mL drainage aid fatty alcohol polyoxiethylene ether, 7.0 g pH regulator triethanolamine, and 2 mL crosslinking agent was added to the mixture. After the mixture was fully stirred, 0.4 g gumming agent ammonium persulfate was added at a certain temperature to make the mixture break for a period of time. After the gumming was completely broken, the mixture was cooled and sealed at room temperature as simulated fracturing flowback fluid.

2.3. Experimental procedure

All experiments were performed in sono-Fenton system, a schematic representation of the setup is depicted in Fig. 1. Each treatment was performed in a 200 mL glass reactor, equipped with water circulating jacket for maintaining reaction temperature to ±1 ℃. Sonication was performed with a sonic processor L500-20 ultrasonic generator (20–25 kHz, 0–600 W, Sonic Systems) equipped with a titanium probe transducer (23820 T). The tip of the horn was 1 cm in diameter and was set at 3.0 cm below the surface of the solution. The ultrasound generator was operated at 40 % duty cycle (4 s on/6 s off). Using calorimetric measurements [49], the actual power dissipated in the system was observed to be 15.7 W for a supplied power of 100 W giving an energy efficiency of 15.7 %. During sonication, 200 mL HPG solutions were poured into the glass reactor, which was placed over a magnetic stirrer for continuous stirring at 390 rpm. Sulfuric acid (10 %) and sodium hydroxide 10 %) solutions were used to adjust the solution's initial pH, which was determined using a pH-meter instrument (Model-PHB-1, China). The temperature of the reaction mixture solution was adjusted using a low-temperature thermostat bath (Ningbo Scientz Biotechnology Co., ltd, Model-SDC-6, China) and monitored by a temperature sensor located inside the reactor. The reaction was started by introducing the US irradiations after adjusting wastewater pH and addition of specific amounts of $FeSO_4{\cdot}7H_2O$ and H_2O_2. Sample with the volume of 15 mL was withdrawn from the reactor at defined time intervals, and immediately adjusted pH to 8 for quenching reaction. The supernatant was used for intrinsic viscosity, chemical oxygen demand (*COD*) and H_2O_2 concentration analysis.

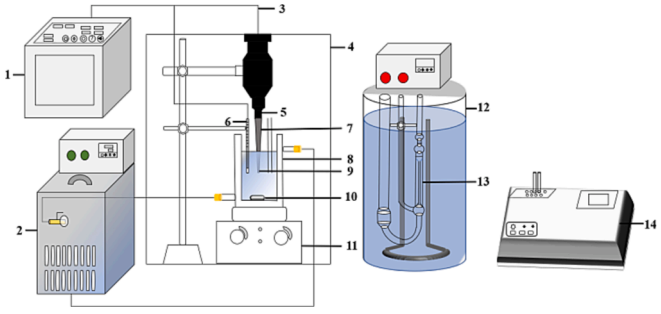

Fig. 1. Schematic diagram of the experimental device. (1) ultrasonic generator; (2) low-temperature thermostat bath; (3) cable; (4) acoustic chamber (5) ultrasonic transducer; (6) temperature sensor; (7) Titanium probe transducer; (8) jacketed glass reactor; (9) ultrasonic probe; (10) magneton; (11) magnetic stirring apparatus; (12) thermostatic water bath; (13) Ubbelohde glass capillary viscometer; (14) water quality tester.

2.4. Analysis

2.4.1. Intrinsic viscosity

The intrinsic viscosity of degraded hydroxypropyl guar gum was measured using Ubbelohde capillary glass viscometer at constant temperature (25 ± 1 ℃). Relative and specific viscosities (η_r and η_{sp}, respectively) were respectively calculated using the following equations:

$$\eta_r = \frac{t}{t_0} \tag{1}$$

$$\eta_{sp} = \eta_r - 1 \tag{2}$$

Where t and t_0 are the efflux time for HPG solution and solvent respectively. The reproducibility for the measurement of efflux time was within 0.3 s. Experiments were repeated twice to check the reproducibility of the obtained data for the variation of concentration against time for all the sets. The experimental errors observed were within ±2 % of the reported average value. The values of the intrinsic viscosity for the degraded HPG solutions were calculated by the one-point intrinsic viscosity equation [50]:

$$[\eta] = \frac{\sqrt{2(\eta_{sp} - \ln\eta_r)}}{C} \tag{3}$$

Where, $[\eta]$ is the intrinsic viscosity (mL/g), c is the concentration of HPG solution (mL/g). The intrinsic viscosity removal rate was calculated using the following equation:

$$[\eta]_{removal} = \left(\frac{[\eta]_0 - [\eta]_t}{[\eta]_0}\right) \times 100\% \tag{4}$$

Where $[\eta]_t$ and $[\eta]_0$ are the $[\eta]$ values at reaction time t and 0, respectively.

2.4.2. Chemical oxygen demand (COD)

COD was determined by the fast digestion-spectrophotometric method, based on the standard methods for the examination of water and waste water [51]. During the *COD* measurement of waste water, residual H_2O_2 in waste water will react with potassium dichromate and affect the determination of the *COD* value [52]. To eliminate this error, this study adopts the following operations to remove the influence of H_2O_2[53]: firstly, adjust the pH of the solution to be tested to 8, and then

residual Fe^{2+} and Fe^{3+} in the solution form precipitation, the supernatant was used for chemical oxygen demand (*COD*) and H_2O_2 concentration analysis. The difference between the measured *COD* value and the *COD* value caused by H_2O_2 in the water sample to be measured was used to characterize the real *COD* value [54]. The *COD* value caused by H_2O_2 is determined according to the working curve of H_2O_2 concentration and *COD* value. A calibration curve was obtained by using the standard H_2O_2 solution with the known concentrations. After linear fitting, the linear equation of *COD* and H_2O_2 concentration can be obtained as follows:

$$y = 13.607x \tag{5}$$

Where, y is the *COD* of H_2O_2 solution, x is H_2O_2 concentration, and the correlation R^2 is 0.999.

The *COD* removal rate was calculated using the following equation:

$$COD_{removal} = \left(\frac{COD_0 - COD_t}{COD_0}\right) \times 100\% \tag{6}$$

Where COD_t and COD_0 are the *COD* values at reaction time t and 0, respectively.

All experiments in this study were performed in triplicate to ensure repeatability error of less than 5 %, and the results presented here represent the average values of three independent measurements.

2.4.3. H_2O_2 concentration

H_2O_2 concentration was determined by measuring the absorbance of potassium titanyl oxalate complex at 405 nm [55]. Prior to the measurement, a calibration curve was obtained by using the standard H_2O_2 solution with the known concentrations, after linear fitting, the linear equation of absorbance and H_2O_2 concentration can be obtained as follows:

$$A = 2.7604C \tag{7}$$

Where, *A* is the absorbance of H_2O_2 solution, *C* is H_2O_2 concentration, and the correlation R^2 is 0.999.

2.4.4. Fe^{2+} concentration

Fe^{2+} concentration was determined by a spectrophotometric method at 510 nm via forming a complex with 1, 10-phenanthroline [56]. Prior to the measurement, a calibration curve was obtained by using the standard Fe^{2+} solution with the known concentrations, after linear fitting, the linear equation of absorbance and Fe^{2+}concentration can be obtained as follows:

$$A = 10.4836C(Fe^{2+}) \tag{8}$$

Where, *A* is the absorbance of Fe^{2+} solution, *C* is Fe^{2+} concentration, and the correlation R^2 is 0.999.

2.4.5. GC–MS analysis

The intermediates of the degradation of HPG by US-Fenton system were identified using GC–MS (Model: Agilent 5977C) with HP-5MS capillary column (30 m × 250 μm × 0.25 μm) film thickness. Helium gas of chromatographic grade was used as carrier gas. The injector temperature was at 300 ℃, the flow rate was 1.0 mL/min and the injection volume was 1 μL. The oven temperature was at 50 ℃ for 1 min, then increased at 8 ℃/min to 280 ℃, and then increased to 290 ℃ at 3 ℃/min with a final hold for 10 min. The electron energy of the ion source (EI) was 70 eV, the transmission line temperature was 320 ℃, and the scan range was 35 to 600 amu.

3. Results and discussion

3.1. Degradation of hydroxypropyl guar gum under different processes

Experiments were performed at the same conditions using US alone, H_2O_2 alone $FeSO_4$ alone, US/ $FeSO_4$, US/ H_2O_2, $FeSO_4$/ H_2O_2, and US/ H_2O_2/ $FeSO_4$ to observe independently the effects on intrinsic viscosity removal and *COD* removal of hydroxypropyl guar gum, and the findings are illustrated in Fig. 2. As shown in the figure, in addition to the $FeSO_4$ treatment alone, other treatment methods reduced the intrinsic viscosity of HPG solution by more than 70 %, while Fenton treatment and US/ Fenton treatment were more than 95 %. Different treatment methods have different degradation mechanisms. In experimental studies on inhibiting ultrasonic degradation of HPG by adding free radical scavenger in our earlier work, it was shown that the ultrasonic degradation of HPG was mainly due to mechanical effects such as intense turbulence and shear caused by ultrasonic cavitation [46]. It is important to note here that the ultrasonic degradation of HPG was only caused by the breakage of glycosidic linkages [47], which led to the degradation of HPG from macromolecule to a small molecular chain. The degradation mechanism of hydrogen peroxide treatment was mainly through the generation of reactive radicals to oxidative HPG. Due to the slow self-decomposition efficiency of H_2O_2 alone, the number of reactive radicals was small, so the intrinsic viscosity removal was less than those of other treatment methods [57]. The intrinsic viscosity only reflected the molecular weight, but not the mineralization degree of HPG. Therefore, *COD* evaluation index was introduced to judge whether different treatment methods meet the waste water discharge standard [58].

As shown in Fig. 2, *COD* removal was less than 5 % when H_2O_2 alone, $FeSO_4$ alone, or ultrasound alone was used. Due to the non-volatile and hydrophilic nature of HPG, degradation reaction would be expected to occur mainly in the bulk solution by radical reaction rather than inside the bubbles by pyrolytic reaction [59]. At a frequency of 20–25 kHz, the concentration of hydroxyl radicals produced in the bulk solution by ultrasound alone was too low to affect the *COD* removal rate. Also, the limited oxidizing power of hydrogen peroxide means that no *COD* removal could be achieved by hydrogen peroxide alone [60]. Nevertheless, ultrasonic cavitation can not only spontaneously generate hydroxyl radicals according to Eqs. (9)–(11) [37], but also promote the decomposition of H_2O_2 into reactive radicals. Higher degradation efficiency of HPG was obtained in US + H_2O_2 system compared with H_2O_2 system, indicating that, due to the complex chemical and physical processes caused by the collapse of cavitation bubble, e.g. thermal decomposition, H_2O_2 decomposed in the cavitation bubble increases the formation of reactive radicals. However, due to the low volatility and high solubility of H_2O_2 in water, the concentration of the H_2O_2 in the cavitation is limited and finally results in a very limited ultrasonic degradation rate of HPG in acidic solution [42].

$$H_2O +))) \rightarrow \cdot OH + \cdot H \tag{9}$$

$$O_2 +))) \rightarrow 2 \cdot O \tag{10}$$

$$\bullet O + H_2O \rightarrow 2 \bullet OH \tag{11}$$

Where“)))” represents ultrasound wave.

The degradation of HPG occurred by Fenton oxidation, the *COD* removal rate was 82.86 %. This is due to hydrogen peroxide interacting with ferrous and ferric ions in acidic solutions to produce reactive radicals such as $^{\bullet}OH/^{\bullet}OOH$ according to Eqs. (12) and (13). The reactive radicals oxidize HPG to produce carbon dioxide and water [36].

$$Fe^{2+} + H_2O_2 + H^+ \rightarrow Fe^{3+} + \bullet OH + H_2O \tag{12}$$

$$Fe^{3+} + H_2O_2 \rightarrow Fe^{2+} + \bullet OOH + H^+ \tag{13}$$

Furthermore, the best *COD* removal result of HPG was received

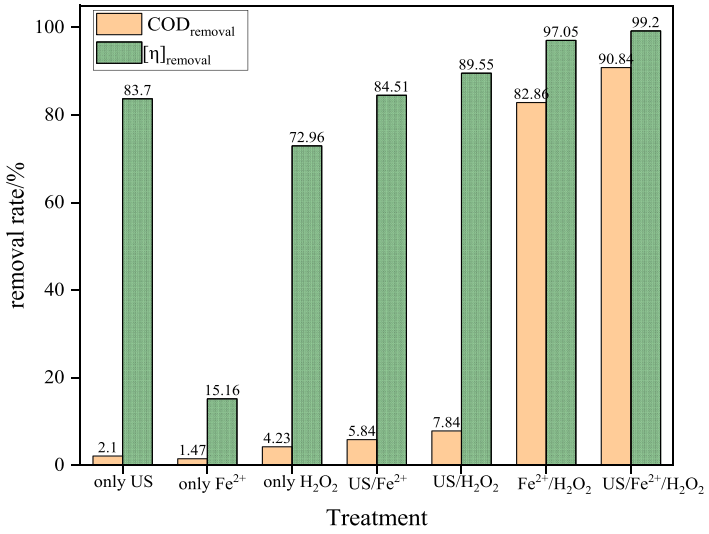

Fig. 2. The performance of various processes in the intrinsic viscosity removal and *COD* removal from HPG (Experimental conditions: pH = 3.0; Temperature = 35 ℃; H_2O_2 concentration = 100 mM, Fe^{2+} concentration = 5 mM, US power = 360 W and treatment time = 60 min).

under US/Fenton treatment, and the *COD* removal rate was 90.84 %. It showed that there were positive synergistic effects between ultrasound and Fenton. In the traditional Fenton reaction, Fe^{3+} was formed according to Eq. (13), and it will react with H_2O_2 and produce a complex intermediate (Fe-O_2H^{2+}) according to Eq. (14). Although Fe-O_2H^{2+} can be decomposed to Fe^{2+} and $^{\cdot}OOH$ spontaneously, the decomposition rate is much smaller. However, combined with the US, the decomposition rate of Fe-O_2H^{2+} can be greatly enhanced (Eq. (15)) [37]. Once the Fe^{2+} was isolated, it reacted with H_2O_2 and produced $^{\cdot}OH$ again, then a cycling mechanism was established. Hence, more $^{\cdot}OH$ can be formed rapidly in the process of US/Fenton and then the best degradation result of HPG was achieved. Meanwhile, the oxygen decomposed by H_2O_2 produces a large number of microbubbles, which can be used as cavitation bubbles of ultrasonic cavitation to enhance the ultrasonic cavitation effect.

$$Fe^{3+} + H_2O_2 \rightarrow Fe - O_2H^{2+} + H^+ \tag{14}$$

$$Fe - O_2H^{2+} + \rightarrow Fe^{2+} + OOH \tag{15}$$

To sum up, to better study the degradation effect of ultrasonic/Fenton and further explore its application prospect and research value, this study explored the effect of different operating parameters on *COD* removal rate based on the US/Fenton treatment.

To further confirm the synergistic effect of degradation of HPG in sono-Fenton system, the synergistic index was calculated as the ratio of rate constant obtained at optimized loading in combined process to the addition of rate constants obtained in the individual process, as represented below:

$$f = \frac{k_{obsA+B+C}}{k_{obsA} + k_{obsB} + k_{obsC}} \tag{16}$$

Where $k_{obsA+B+C}$, k_{obsA}, k_{obsB} and k_{obsC} are the observed rate constants (min^{-1}) of system A + B + C, system A, system B, system C, respectively.

According to the above formula, the synergistic indexes of US/Fe^{2+}, US/H_2O_2, Fe^{2+}/H_2O_2 and US/ Fe^{2+}/H_2O_2 were 1.83, 2.11, 16.43 and 20.45, respectively. The extreme high f (20.45) demonstrates the extreme strong synergistic effect of degradation of HPG in US/Fe^{2+}/H_2O_2 system.

3.2. Effects of important parameters on the degradation of HPG

3.2.1. Effect of reaction time

Fig. 3 illustrates the *COD* removal rate of HPG at different reaction times when H_2O_2 concentration was 100 mM, $FeSO_4$ concentration was 5 mM, pH was 3.0, temperature was 35 ℃ and ultrasonic power was 360 W. It was observed that the *COD* removal rate of HPG increased rapidly

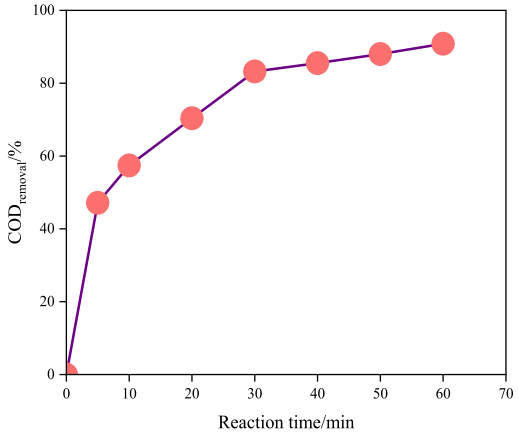

Fig. 3. The effect of reaction time on the *COD* removal rate of HPG (Experimental conditions: pH = 3.0, Temperature = 35 ℃, H_2O_2 concentration = 100 mM, Fe^{2+} concentration = 5 mM and US power = 360 W).

to reach 47.15 % during the first 5 min, 83.23 % at 30 min, and then increased slowly to 90.84 % in 60 min, respectively. It means that organic materials were rapidly degraded by sono-Fenton reaction. Most organic removals occurred in the first 30 min. After 30 min, the change in residual *COD* became insignificant. More foam was observed on the top layer of HPG solutions as the oxidation proceeded. This was evidence of carbon dioxide formation. In another study, different researchers observed a similar trend in the removal of a wide range of pollutants such as polyacrylamide (PAM) [61] and extracellular polymeric substances (EPS) [62]. It means that the trend of the degradation of polymers by sono-Fenton is quite consistent over time, which provides a good basis for the study of kinetics.

Residual ferrous iron and hydrogen peroxide was measured during Fenton reaction, and the results are shown in Fig. 4. It can be seen that most of the Fenton's reagent was consumed in the first 10 min. Residual ferrous iron and hydrogen peroxide decreased from 5 mM to approximately 1.02 mM, and 100 mM to approximately 10.85 mM, respectively. It means that there was a violent chemical reaction in the whole sono-Fenton reaction system in the first 10 min. During this period, a great deal of ˙OH radical was generated to oxidize HPG, meanwhile, the structure of HPG was changed and a multitude of reaction intermediates was produced. The *COD* removal rate of HPG was relatively large within 30 min. It seems that the chemical reaction continued rapidly during this period, and HPG was oxidized to carbon dioxide, water, and other inorganic substances. However, after 30 min, due to the small amount of H_2O_2 remaining, the *COD* removal rate of HPG rate was stabilized. During this period, the degradation efficiency was weakened, although the chemical reaction was still going on.

Based on the results, the reaction time for the sono-Fenton treatment was determined to be 30 min for further experiments.

3.2.2. *Effect of the H_2O_2 concentration*

In the US/Fenton system, hydrogen peroxide as the dominant source of ˙OH has always been a critical parameter [63]. The *COD* removal rate of HPG at different concentrations of H_2O_2 (0–120 mM) was investigated at reaction time of 30 min, temperature of 35 ℃, $FeSO_4$ concentration of 5 mM, pH of 3.0, and US power of 360 W and obtained results are depicted in Fig. 5. It was observed that the *COD* removal rate increased from 5.84 % to 83.23 % as a consequence of increasing the H_2O_2 concentration from 0 mM to 100 mM, respectively. It means that the *COD* removal rate of HPG increases with the increase of H_2O_2 dosage in a certain range, and that the results were consistent with the previous studies about degradation of HPG using sono-Fenton reactions [64]. It is evident that hydrogen peroxide interacts with ferrous and ferric ions in acidic solutions to produce reactive radicals such as ˙OH according to Eqs. (17) and (18). Another reason for the results may be that the increase of H_2O_2 concentration will continuously reduce the surface tension of the liquid, thus reducing the ultrasonic cavitation threshold, generating more cavitation events and promoting the generation of hydroxyl radicals according to Eq. (9) [65]. However, it should be noted that further increase in the concentration of H_2O_2 causes a decrease in the *COD* removal rate, the *COD* removal rate decreased from 83.23 % to 80.95 % as a consequence of increasing the H_2O_2 concentration from 100 mM to 120 mM. This can be explained because excess H_2O_2 may act as a scavenger for ˙OH resulting in the generation of hydroperoxy radicals (Eq. (16)) that are less reactive than the hydroxyl radicals [57]. At these higher H_2O_2 concentrations, hydroxyl radicals react with the peroxide in preference to the HPG so the degradation rate is reduced.

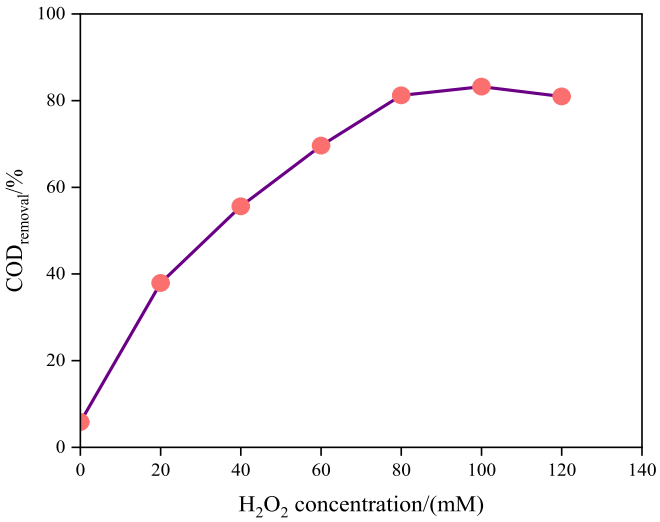

Fig. 5. The effect of H_2O_2 concentration on the *COD* removal rate of HPG (Experimental conditions: pH = 3.0, Temperature = 35 ℃, Fe^{2+} concentration = 5 mM, US power = 360 W and Reaction time = 30 min).

$$H_2O_2 + \cdot OH \rightarrow H_2O + HO_2 \quad (17)$$

$$HO_2\cdot + \cdot OH \rightarrow H_2O + O_2 \quad (18)$$

Therefore, based on both cost and degradation efficiency, 80 mM was selected as an optimum concentration of H_2O_2 for the *COD* removal rate of HPG by US/Fenton system. It is notable that the concentration of hydrogen peroxide (80 mM) used here was lower than that used in previously published studies (500 mM) [64], which indicates that ultrasound may be applied at lower concentration than previously suggested and is very useful in minimizing the amount of reagent necessary for HPG treatment.

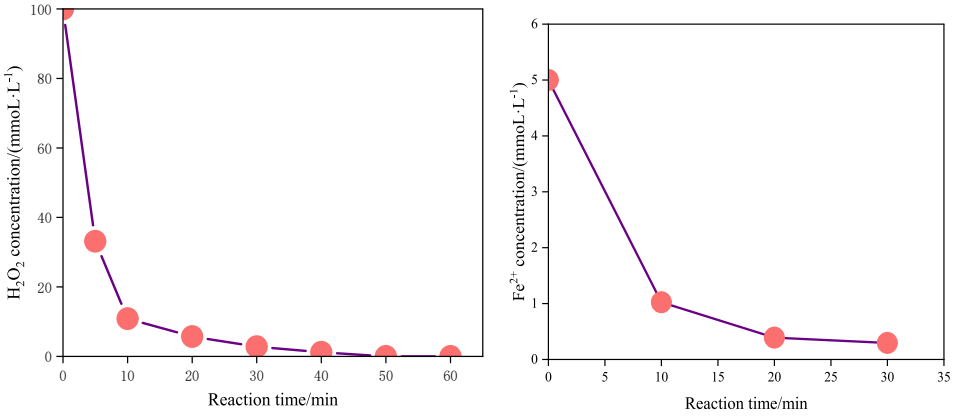

Fig. 4. (a) H_2O_2 concentration change diagram; (b) Fe^{2+}concentration change diagram (Experimental conditions: pH = 3.0, Temperature = 35 ℃, H_2O_2 concentration = 100 mM, Fe^{2+} concentration = 5 mM and US power = 360 W).

3.2.3. Effect of Fe^{2+} concentration

Fe^{2+} concentration is one of the crucial operating parameters that determine the treatment efficiency and operating costs of the sono-Fenton process. Fig. 6 shows the influence of Fe^{2+} concentration on the *COD* removal rate of HPG by sono-Fenton. It was observed that the degradation of HPG was significantly influenced by Fe^{2+} concentration and distinctly increased with the increasing amount of Fe^{2+}. The *COD* removal rate increased from 5.84 % to 82.27 % as a consequence of increasing Fe^{2+} dosage from 0 to 9 mM. This is because Fe^{2+} acts as a catalyst and initiates the decomposition of H_2O_2 to produce the reactive $^{\bullet}OH$ radical according to Eqs. (12) and (13). More $^{\bullet}OH$ radicals were generated with the increase of Fe^{2+} concentration, thereby increasing the efficiency of *COD* removal [36]. However, the *COD* removal rate decreased from 82.27 % to 79.07 % as a consequence of increasing Fe^{2+} dosage from 9 to 13 mM. This is because a greater concentration of Fe^{2+} can cause the recombination of radical $^{\bullet}OH$, resulting in the reduction of *COD* removal efficiency, the excess Fe^{2+} reacts with the $^{\bullet}OH$ radical functioning as a scavenger according to Eq. (19) [66]. In contrast to Zhang's Fenton degradation of hydrolyzed polyacrylamide [67], the present manuscript reduced the range of Fe^{2+} concentration. It is notable that the concentration of Fe^{2+} (37.5 mM) used in Lei's study was higher than that in this manuscript. However, the high concentration of Fe^{2+} would cause the recombination of hydroxyl radicals and produce more sludge pollutants.

$$Fe^{2+} + \bullet OH \rightarrow Fe^{3+} + OH^- \quad (19)$$

In industrial applications, to reduce the production of sludge from iron complex and acquire the maximum *COD* removal efficiency, it is desirable that the amount of iron used must be optimum. Therefore, 5 mM of Fe^{2+} concentration was selected as an optimum dosage for the degradation of HPG by US/Fenton.

3.2.4. Effect of the ultrasonic power

To make a clear description of the effect of ultrasound irradiation on the degradation of HPG by sono-Fenton, a series of experiments were carried out at different ultrasonic power (0–540 W), and the results are shown in Fig. 7. It can be seen that the *COD* removal rate increased from 73.74 % to 80.79 % as a consequence of increasing ultrasonic power from 0 to 180 W. It means that the ultrasound further enhances the Fenton process in degrading HPG. This has commonly been reported in sono-chemical systems [68]. The number of ultrasonic cavitation events

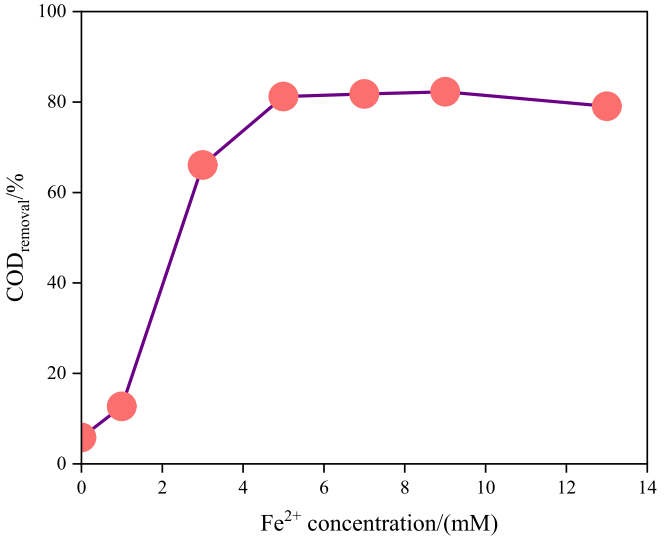

Fig. 6. The effect of Fe^{2+} concentration on the *COD* removal rate of HPG (Experimental conditions: pH = 3.0, Temperature = 35 ℃, H_2O_2 concentration = 80 mM, US power = 360 W and Reaction time = 30 min).

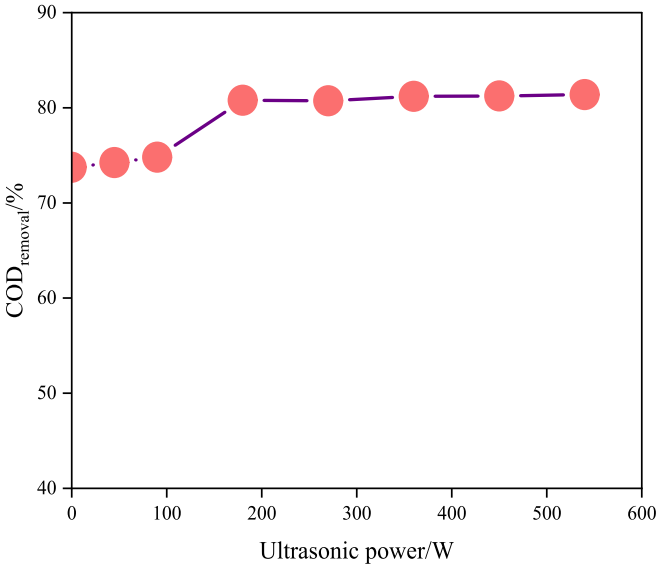

Fig. 7. The effect of ultrasonic power on the *COD* removal rate of HPG (Experimental conditions: pH = 3.0, Temperature = 35 ℃, H_2O_2 concentration = 80 mM, Fe^{2+} concentration = 5 mM and Reaction time = 30 min).

occurring in the sono-Fenton system increases with an increase in the ultrasonic power [69], and the increase of cavitation events would enhance the mechanical shear force generated by the collapse of cavitation bubbles and increase the number of hydroxyl-free radicals, hence the *COD* removal rate of HPG would also increase accordingly. However, it can be observed that the *COD* removal rate of HPG stabilized after the ultrasonic power exceeded 180 W. It could be assumed that there were two fundamental factors contributing to this phenomenon. It can be suggested that as the number of cavitation bubbles will gradually increase with the increase of power, cavitation bubbles would be "excessive" after reaching a certain degree. These excessive cavitation bubbles would make the sound wave reflected to the emitter or scattered to the container wall, resulting in the air screen effect, which will have a certain effect on the degradation process [70]. Another reason for the phenomenon may be the high heat and high pressure (5000 K, 100 MPa) generated instantaneously by the ultrasonic cavitation bubble collapsing, leading to the decomposition of hydrogen peroxide, which cannot fully react with Fe^{2+} [71]. And hence, $^{\bullet}OH$ free radical generation is reduced, which limits the *COD* removal rate effect of HPG. In contrast to Amrutlal ultrasonic degradation of guar gum [72], ultrasonic power was not the most important parameter in guar gum degradation using sono-Fenton process, ultrasound functioned to enhance the Fenton process. A low intensity of ultrasonic energy was sufficient to achieve the rapid breaking of molecular chains, but has little effect on the reduction of *COD*. Hence, the study shows that ultrasound only acts as an auxiliary means in the process of sono-Fenton process, and the *COD* removal of HPG mainly relies on Fenton reaction. Therefore, the ultrasonic power of 180 W is the optimum reaction condition to both save energy and increase the degradation efficiency.

3.2.5. Effect of initial pH

The initial pH of the solution is one of the most critical factors influencing Fe^{2+} concentrations and the production of $^{\bullet}OH$ radical in the sono-Fenton system [73]. The effect of the initial pH on the degradation of HPG by sono-Fenton was investigated and the results are shown in Fig. 8. It was observed that the *COD* removal rate of HPG solution was significantly influenced by the initial pH and the highest degradation efficiency was achieved at pH 2.5. The *COD* removal efficiency increased from 67.31 % to 81.18 % as a consequence of the pH decreasing from 6.0 to 2.5. It is conceivable that the acidic pH is beneficial for the degradation of HPG. Ozkan et, al. [57] have also reported the oxidation

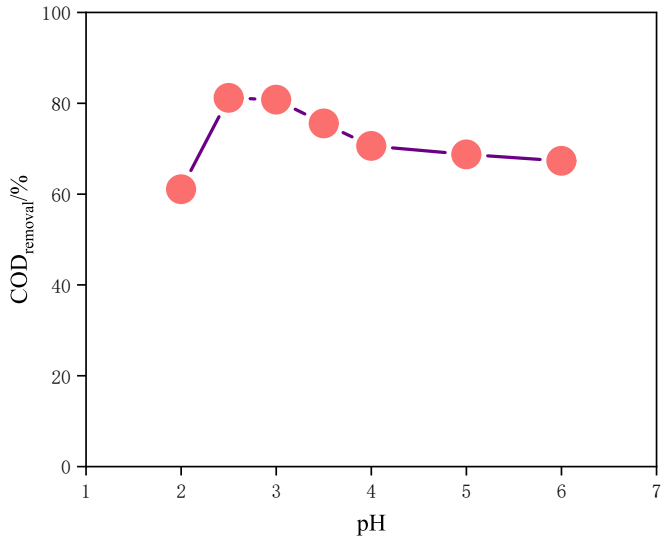

Fig. 8. The effect of ultrasonic power on the *COD* removal rate of HPG (Experimental conditions: Temperature = 35 ℃, H_2O_2 concentration = 80 mM, Fe^{2+} concentration = 5 mM, ultrasonic power = 180 W and Reaction time = 30 min).

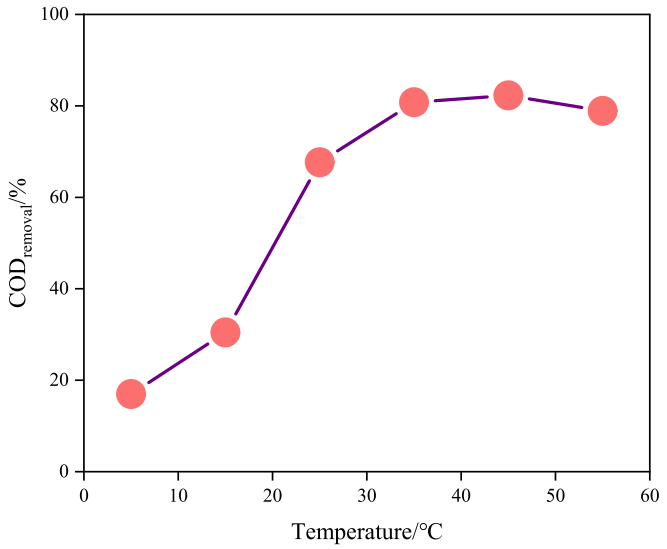

Fig. 9. The effect of ultrasonic power on the *COD* removal rate of HPG (Experimental conditions: pH = 3.0, H_2O_2 concentration = 80 mM, Fe^{2+} concentration = 5 mM, ultrasonic power = 180 W and Reaction time = 30 min).

potential of ·OH/H_2O decreased from 2.59 to 1.65 V vs standard hydrogen electrode (SHE) with increasing the pH from 0 to 14. However, lower pH was not always better, decreasing the pH from 2.5 to 2.0 will make the *COD* removal rate efficiency decrease from 81.18 % to 61.06 %. When pH < 2.5, the excess H^+ reacts with the ·OH radical functioning as a scavenger according to Eq. (20). In addition, Hydrogen peroxide could capture H^+ and form an oxonium ion ($H_3O_2^+$) at the lower pH according to Eq. (21), $H_3O_2^+$ would make hydrogen peroxide electrophilic and enhance its stability, which potentially reduces the reactivity of hydrogen peroxide reaction with ferrous ions[37].When pH > 4.0, Fe^{2+}/Fe^{3+} would precipitate in the formation of hydroxide which cannot fully catalyze H_2O_2 reaction to generate ·OH radical, resulting in the degradation efficiency decrease. Another contributing factor may be the decrease of the oxidation potential of ·OH in the higher pH resulting in the decrease of *COD* removal rate efficiency. In contrast to Nannan ultrasonic degradation of polyacrylamide [61], the pH range of HPG degraded by ultrasound-Fenton in this paper was larger, and the *COD* removal rate still maintained a higher range when the pH reached 6. When pH of the HPG solution treated by ultrasound-Fenton was measured, it was found that the pH value of the solution dropped from 6 to about 2.5, indicating that the sono-Fenton treatment of HPG produces H^+, which changes the initial pH value. Therefore, sono-Fenton degradation has no strict selectivity for pH value. It is beneficial for ultrasonic treatment of waste liquid with wide pH range. The *COD* removal rate of HPG difference between pH 3.0 and pH 2.5 was only 0.39 %, hence the optimum pH should be 3.0 in terms of cost-effectiveness for practical applications.

$$H^+ + \cdot OH + e^- \rightarrow H_2O \tag{20}$$

$$H_2O_2 + H^+ \rightarrow H_3O_2^+ \tag{21}$$

3.2.6. Effect of temperature

We explored the effect of temperature on the degradation of HPG in the sono-Fenton system since it was considered a crucial factor to regulate the reaction rate in chemical processes, and the findings are illustrated in Fig. 9. The results showed that the degradation of HPG increased with the increase of temperature. The *COD* removal rate of HPG increased from 16.98 % to 82.30 % as a consequence of increasing the temperature from 5 ℃ to 45 ℃ within 30 min. It could be speculated that the temperature was critical to the reaction rate and it influenced the degradation efficiency greatly. On the one hand, the rate of the redox reaction could be accelerated by increasing the temperature. So, in the sono-Fenton system, the higher the temperature is, the faster the reaction rate is between hydrogen peroxide and ferrous iron, thereby increasing the rate generation of ·OH radical as well as the degradation rate of HPG [74]. On the other hand, the surface tension of water decreases with the temperature. According to Eq. (22) [75], the decrease of surface tension will reduce the energy barrier for nucleation, which is conducive to the generation of more cavitation bubbles. Therefore, the increase in temperature would strengthen the ultrasonic cavitation reaction and produce more ·OH within a certain temperature range. However, there was a remarkable decline in the degradation efficiency when the temperature continued to rise to 55 ℃. For this reason, excessively high temperatures can result in the precipitation of ferrous iron and self-decomposition of H_2O_2 [76], which would reduce the sono-Fenton reaction rate and the degradation efficiency of HPG. Moreover, higher temperature is likely to facilitate bubble formation due to an increase of the equilibrium vapor pressure in the sono-Fenton system. Nevertheless, bubbles with more vapors would buffer the implosion process. Thus, the maximum temperature upon bubble collapse will decrease, which reduces the cavitation effect and lowers the rate of chemical reaction [77]. Different from previous studies [78], this study has a higher requirement on temperature, and the *COD* removal rate was only 16.98 % when the temperature was 5℃. The *COD* removal rate of HPG difference between temperature 35 ℃ and temperature 45 ℃ was only 1.15 %, hence the optimum temperature should be 35 ℃ in terms of cost-effectiveness for practical applications.

$$E = \frac{16\pi\sigma^3}{3P^2} \tag{22}$$

Where, E is the energy barrier against nucleation, σ is the macroscopic surface tension of the solution, and P is a negative pressure in the liquid solution.

3.3. Kinetic studies

Kinetic study on degradation of HPG was investigated using sono-Fenton system under optimum conditions above. In the study, the kinetic model derived by Chan et al. [79] was used to simulate the reaction kinetics. The kinetic equation is given as follows:

$$\frac{C}{C_0} = 1 - (\frac{t}{m + bt}) \quad (23)$$

where C_0 is the initial concentration of HPG (mg/L); C is the concentration at time (t) (mg/L); m and b are the two dimensionless characteristic constants of the model relating to the initial removal rate and maximum oxidation capacities, respectively.

Since various initial concentrations of HPG had different *COD*, which showed a linear relationship, *COD* was used to replace the concentration of the above kinetic model. The adjusted kinetic model is as follows:

$$\frac{COD}{COD_0} = 1 - (\frac{t}{m + bt}) \quad (24)$$

where COD_0 is the initial *COD* of HPG (mg/L); C is the *COD* at the time (t) (mg/L).

Eq. (24) can be linearized to obtain Eq. (25):

$$\frac{t}{1 - \frac{COD}{COD_0}} = m + bt \quad (25)$$

The sono-Fenton reaction kinetics under optimal conditions was described by drawing the relation between t /(1-COD/COD_0) and t, where m and b are intercept and slope, and the results are illustrated in Fig. 10. It was observed that the degradation of HPG followed strictly to two-stage reaction kinetics ($R^2 > 0.99$). Meanwhile, first-order, second-order, and Chan kinetic models were used to simulate the degradation of HPG by sono-Fenton system under optimal conditions, and the comparison results are shown in Table 1. According to the results, the degradation of HPG by sono-Fenton process correlated closer to the Chan kinetic models ($R^2 > 0.99$) but less close to first-order kinetics ($R^2 = 0.6863$) based on comparing R^2. And hence, it was concluded that the two-stage kinetic model was suitable for the degradation of hydrophilic HPG in sono-Fenton processes.

3.4. Intermediates analysis

The degradation products of HPG treated by sono-Fenton for 10 min, 20 min, and 30 min were characterized by GC–MS, and the results showed that several intermediate peaks appeared after 10 min degradation, while the peaks for either HPG or its degradation intermediates were weakened nearly 10-fold after 20 min and 30 min. It indicates that not only HPG but also the intermediates products could be degraded

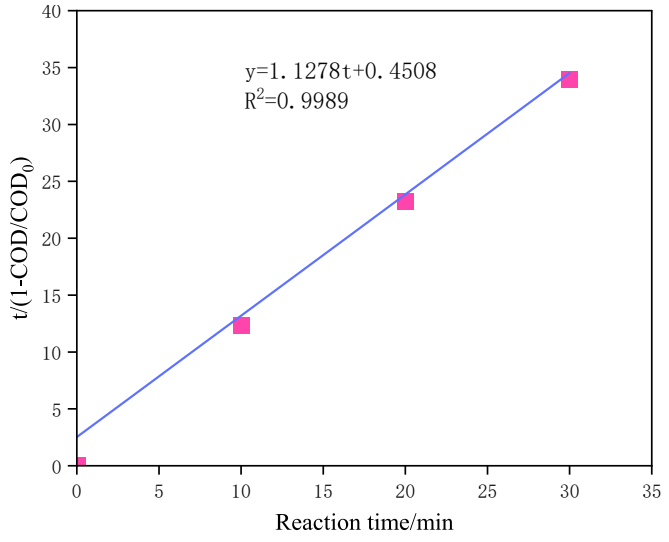

Fig. 10. Relationship between $t/(1 - C/C_0)$ and oxidation time t in sono-Fenton processes under optimum conditions(Experimental conditions: pH = 3.0, temperature = 35 ℃, H_2O_2 concentration = 80 mM, Fe^{2+} concentration = 5 mM, ultrasonic power = 180 W and Reaction time = 30 min).

Table 1
The equations and R^2 of the kinetic models.

Reaction order	The linearized reaction equation	R^2
First	$\ln C = \ln C_0 - kt$	0.6863
Second	$1/C = 1/C_0 + kt$	0.8947
Chan Kinetic Model	$t/(1 - C/C_0) = m + bt$	0.9989

efficiently in sono-Fenton process.

According to the molecular ion mass and MS/MS fragmentation patterns, the molecular structure of each identified product was proposed by comparing the MS data with the highest matching degree given by the NIST atlas library. Based on the product analysis, possible degradation pathways are also proposed as represented in Fig. 11.

It was speculated that the degradation process of HPG was mainly divided into two steps, the first step was the chain breaking process of HPG, the second step was the small molecular chain oxidation process. Under the action of ultrasonic cavitation of hydroxypropyl guar gum, the α-1,6 glycoside bond and β-1,4 glycoside bond break first, which degraded HPG from polymer to small molecule six-membered ring compound. When the degradation of HPG main chain reached a certain extent, C—C bonds such as C_2, C_3, C_4 and C_6 on the main chain begin to break. As the reaction continues, these ring structures were gradually degraded to produce structural fragments with correspondingly smaller molecular weights. Subsequently, two possible degradation pathways could be concluded to initiate the degradation of these structural fragments as a result of the attack by ultrasonic cavitation and ˙OH radicals. The first possible pathway was that these small molecular structure fragments were converted into aromatic compounds, including naphthalene, dimethyl phthalate, 1,2,3,4-tetrahydro-naphthalene were observed in treated HPG in detectable amounts, which have a benzene ring in their structure. Subsequently, the benzene ring was attacked by ˙OH and gradually degraded into smaller units, such as 1,2,3-trimethyl-benzene, 1-ethyl-4-methyl-benzene and 1-ethyl-4-methyl-benzene. The second possible pathway was that these small molecular structure fragments were converted into aliphatic compounds, including hexadecane, tridecane, dodecane, undecane, decane and nonane. Subsequently, the carbon chain fatty alcohol was attacked by ˙OH and gradually degraded into smaller units. However, identification of all developed intermediates is not possible, because of their slight accumulation and the limitations associated with the GC–MS analytical technique. Hence, most of unknown intermediates were gradually mineralized into CO_2 and H_2O by oxidation of ˙OH radicals. It is noticeable that sono-Fenton system provides a favorable condition for discharging studied fracture flowback fluid in terms of environmental standards and legislation. According to the results, sono-Fenton process can be applied as a promising advanced treatment approach for effective treatment of refractory fracture flowback fluid.

3.5. Scavenging effect and mechanism research

To elucidate HPG degradation mainly caused by pyrolysis or radical oxidation in the sono-Fenton system, *n*-butanol, EDTA-2Na, and BQ were used to scavenge hydroxyl radicals in sono-Fenton system under optimum conditions above. The employed scavengers were *n*-butanol, EDTA-2Na, and BQ for ˙OH, H^+, and $O_2^{\cdot-}$; respectively [80]. A removal efficiency of 83.23 % was also obtained, since the reaction could be completed in the absence of any scavenger. The removal efficiency, however, declined to 5.07 %, 54.24 %, and 45.27 % in the presence of *n*-butanol, EDTA-2Na, and BQ, respectively (Fig. 12). It was observed that various impacts of the decomposition rate by addition of scavengers had followed the order of EDTA-2Na < BQ < *t*-BuOH. So, the main mechanism of HPG in the sono-Fenton system was not the high-temperature pyrolysis in the cavitation bubbles, nor the mechanical shear force, but the oxidation reaction of ˙OH radical.

Regarding the results of quenching tests, a possible mechanism for

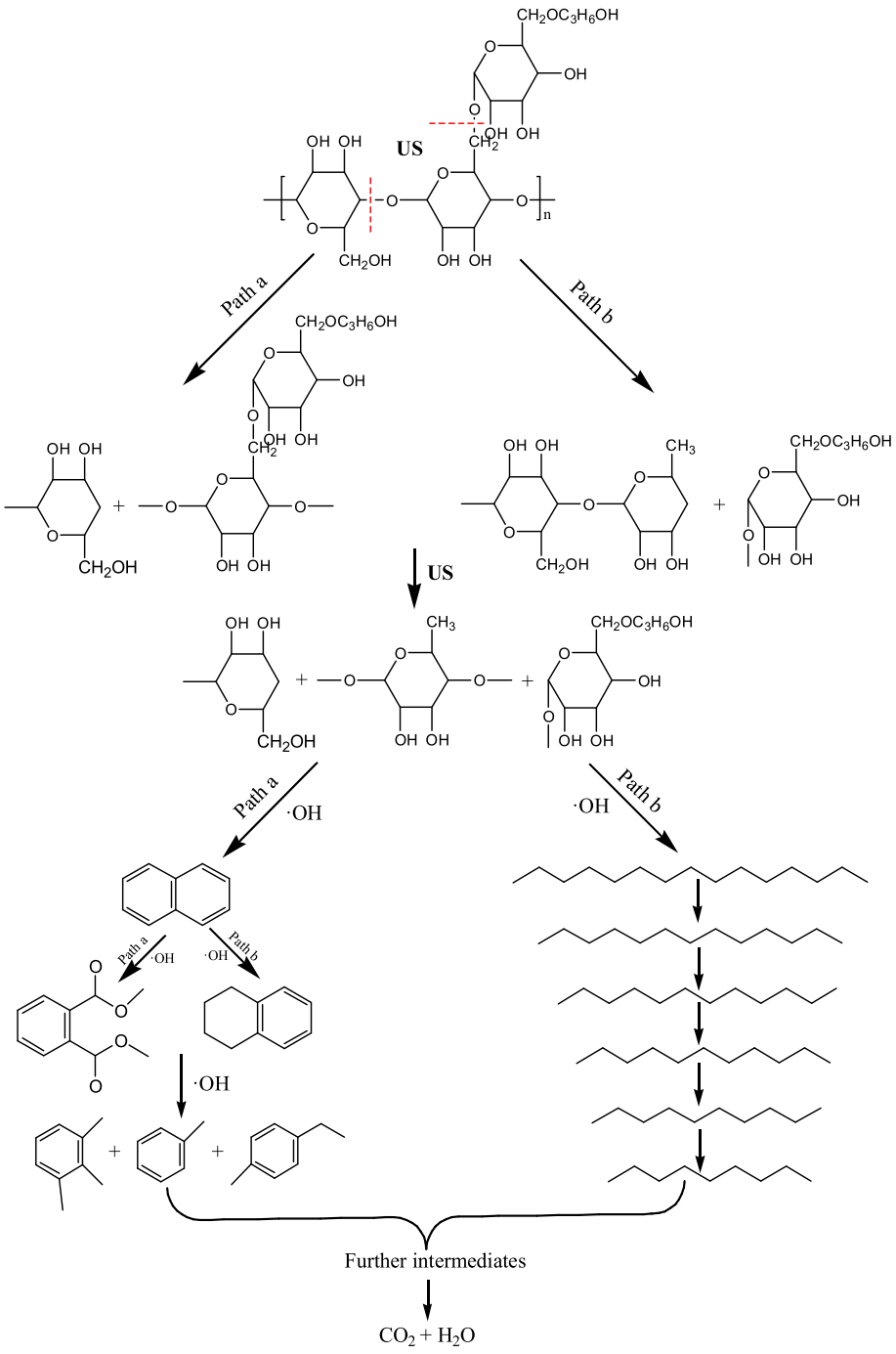

Fig. 11. Proposed pathways of HPG degradation based on GC–MS analysis.

HPG degradation over sono-Fenton system was pointed out in Fig. 13. The proposed pathways of HPG degradation in the sono-Fenton system are briefly summarized as follows.

(1) Cavitation bubbles will undergo collapse and expansion in the oscillating pressure field, and implode when the bubbles reach unstable size. During the bubbles collapse, high temperature causes the decomposition of water and oxygen molecules in the bubbles to generate a variety of oxides, such as·OH, H_2O_2, ·H, ·O (Eqs. (1)–(3)) [81]. Most of ·OH and ·H recombine in the interior region, and the rest of ·OH are diffused to the gas–liquid interface region, where they will recombine to H_2O_2 or react with HPG.

(2) Degradation mechanism of organic compounds in traditional homogeneous Fenton system. In the liquid region, hydrogen peroxide interacts with ferrous and ferric ions in acidic solutions to produce reactive radicals such as ·OH/·OOH according to Eqs. (5) and (6). The reactive radicals oxidize HPG to produce carbon dioxide and water (Eq. (7)).

(3) The synergistic mechanism of ultrasound and Fenton is as follows: the strong shear force generated by the implosion of cavitation bubbles would promote the decomposition of H_2O_2 in Fenton system to produce oxygen. Oxygen could be used as a cavitation bubble of ultrasonic cavitation to enhance the ultrasonic cavitation effect. Furthermore, ultrasound could improve the decomposition rate of Fe-O_2H^{2+} and establish a cycling

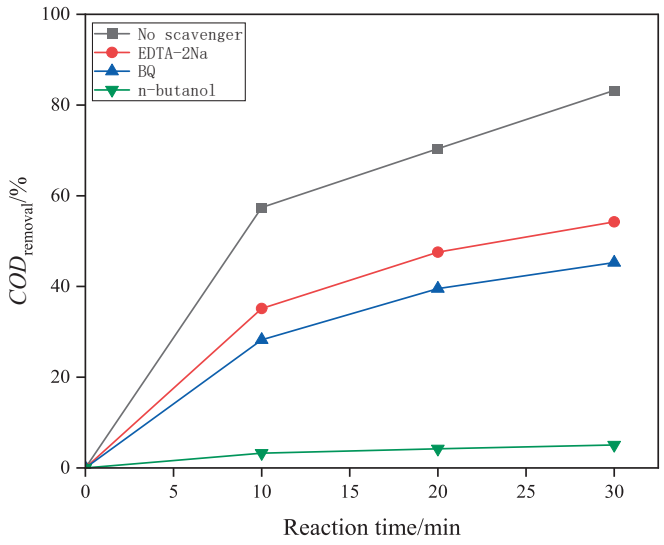

Fig. 12. Effect of different scavengers on HPG degradation at optimum conditions (Experimental conditions: pH = 3.0, temperature = 39 ℃, H_2O_2 concentration = 87 mM, Fe^{2+} concentration = 6 mM, ultrasonic power = 180 W, scavenger = 5 mM and reaction time = 30 min).

mechanism of continuous generation of ˙OH, to obtain a better degradation effect of HPG. In addition, the shear force generated by ultrasonic cavitation is conducive to the chain breaking of HPG into small molecules, thus increasing the surface area of pollutants and making them better contact with ˙OH produced by Fenton reaction, to be degraded into CO_2 and water.

3.6. Treatment of simulated fracture flowback fluid

In order to verify the field application of the sono-Fenton system on fracturing flowback fluid, this manuscript prepared a simulated fracturing flowback fluid with seawater from the Yellow Sea as the solvent. The *COD* value was determined to be 25802.80 mg/L, and the *COD* value was 675.21 mg/L after 40 times dilution. Study on degradation of diluted fracture flowback fluid was carried out using sono-Fenton system under optimum conditions above. The *COD* of the simulated fracturing flowback fluid decreased to 144.23 mg/L, 107.78 mg/L and 80.83 mg/L, respectively, after degradation for 30 min, 45 min and 60 min, indicating that the seawater based fracturing flowback treated by this system under the optimal conditions could fully meet the marine sewage discharge standards.

3.7. Energy consumption

The energy consumption is mainly electric energy, which comes from the constant temperature water bath and ultrasonic generator. Thus, the energy consumption based on sono-Fenton system was found to be 0.83 kW/h under optimum condition such as the pH of 3.0, the H_2O_2 concentration of 80 mM, the Fe^{2+} concentration of 5 mM, the ultrasonic power of 180 W, the ultrasonic frequency of 20–25 kHz, the temperature of 39 ℃ and the reaction time of 30 min.

4. Conclusion

This study shows that there are positive synergistic effects between ultrasound and Fenton. Results of quenching test shows that ˙OH radicals have a dominant role in destructing the HPG. Based on a kinetic study, it is concluded that Chan Kinetic Model is more appropriate to describe the degradation of HPG. Finally, GC–MS is used for the identification of some degradation intermediates, and the results shows that the intermediates contain a large number of aromatic compounds with benzene rings and aliphatic compounds.

The results obtained from the present study indicates that the homogeneous sono-Fenton process can be used effectively for removing HPG from fracture flowback fluid. However, sono-Fenton treatment technology still has some limitations. Its main disadvantage is to control pH to prevent $Fe(OH)_3$ precipitation. Heterogeneous catalysts (magnetite, hematite, and pyrite) can be used to overcome the problems of the sono-Fenton process.

CRediT authorship contribution statement

Fuhua Wang: Validation, Visualization, Investigation, Conceptualization, Formal analysis, Funding acquisition, Project administration, Resources, Supervision, Writing – review & editing. **Zezhuang Sun:** Data curation, Software, Formal analysis, Investigation, Methodology, Visualization, Writing – original draft, Writing – review & editing. **Xian Shi:** Data curation, Investigation, Funding acquisition, Resources. **Luyi Wang:** Data curation, Formal analysis, Investigation. **Weidong Zhang:**

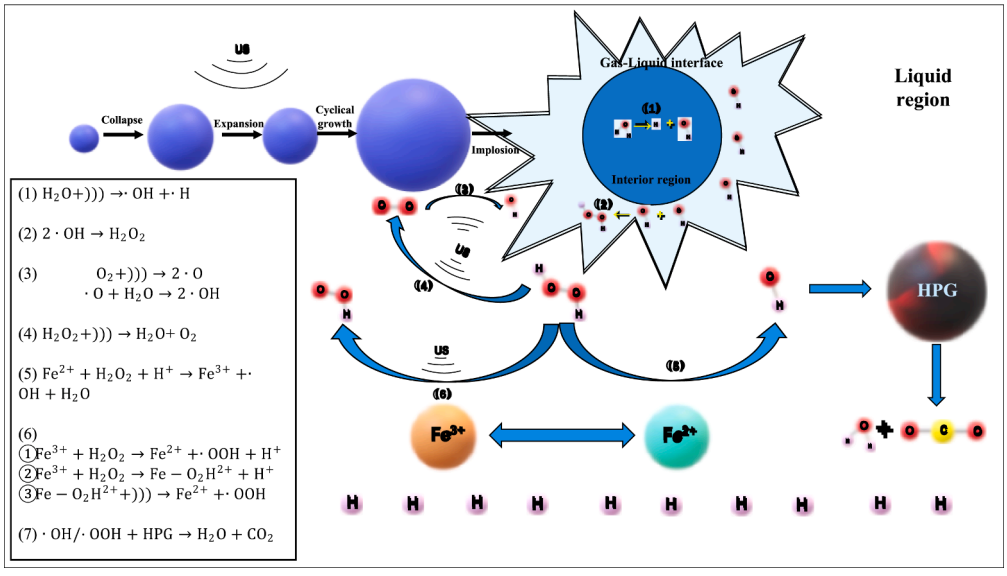

Fig. 13. Proposed schemes for generation of reaction free radicals and degradation of HPG during sono-Fenton treatment.

Data curation, Formal analysis, Investigation. **Zhihao Zhang:** Data curation, Formal analysis, Investigation.

Declaration of Competing Interest

The authors declare that they have no known competing financial interests or personal relationships that could have appeared to influence the work reported in this paper.

Acknowledgment

The authors thank the China University of Petroleum (East China) for all the support. This work was supported by Shandong Province's key RESEARCH and development program "Seawater based fracturing flowback fluid ultrasonic degradation mechanism and key technology" (2019GGX103009).

References

[1] B. Goodman, J.A. Cohen, M.F. Levitt, et al., Environmental issues and answers related to shale gas development, Am. J. Phys. Anthropol. 206 (2015) 1123, https://doi.org/10.2118/174164-MS.
[2] Andrew, Kondash, Avner, et al. Water footprint of hydraulic fracturing. Environ. Sci. Technol. Lett., 2015, 2(10): 276-280. 10.1021/acs.estlett.5b00211.
[3] Hollanda L R, Santos S B F, Faustino, et al. Oil field–produced water treatment: characterization, photochemical systems, and combined processes. 2021, 28(38): 52744-52763. 10.1007/s11356-021-16222-1.
[4] Feng Z, Hz B, Xl B, et al. Enhanced remediation of fracturing flowback fluids by the combined application of a bioflocculant/biosurfactant-producing Bacillus sp. SS15 and its metabolites. Chemosphere, 2022, 302: 134870. https://doi.org /10.1016/j. chemosphere.2022.134870.
[5] J.Y. Guo, Evaluation of Retarded Crosslinked Polymer Fracturing Fluid, Daqing Petroleum Institute, 2007.
[6] Hammer R, VanBriesen, J. In fracking's wake: New rules are needed to protect our health and environment from contaminated wastewater. Natural Resources Defense Council (NRDC), 2012, 11. http://www.nrdc.org/energy/files/fracking-wastewater-fullreport.pdf.
[7] K.A. Sitterley, J.A. Silverstein, J. Rosenblum, et al., Aerobic biological degradation of organic matter and fracturing fluid additives in high salinity hydraulic fracturing wastewaters, Sci. Total Environ. 758 (2020), 143622, https://doi.org/10.1016/j.scitotenv.2020.143622.
[8] A. Butkovskyi, H. Bruning, S.A. Kools, et al., Organic Pollutants in Shale Gas Flowback and Produced Waters: Identification, Potential Ecological Impact, and Implications for Treatment Strategies, Environ. Sci. Tech. 51 (9) (2017) 4740–4754, https://doi.org/10.1021/acs.est.6b05640.
[9] J.M. Estrada, R. Bhamidimarri, A review of the issues and treatment options for wastewater from shale gas extraction by hydraulic fracturing, Fuel 182 (oct.15) (2016) 292–303, https://doi.org/10.1016/j.fuel.2016.05.051.
[10] A. Abramowska, D.K. Gajda, K. Kiegiel, et al., Purification of flowback fluids after hydraulic fracturing of Polish gas shales by hybrid methods, Sep. Sci. Technol. 53 (8) (2018) 1207–1217, https://doi.org/10.1080/01496395.2017. 1344710.
[11] D.E. Freedman, S.M. Riley, Z.L. Jones, et al., Biologically active filtration for fracturing flowback and produced water treatment, J. Water Process Eng. 18 (2017) 29–40, https://doi.org/10.1016/j.jwpe.2017.05.008.
[12] C.L. Conrad, Y. Ben Yin, T. Hanna, et al., Fit-for-purpose treatment goals for produced waters in shale oil and gas fields, Water Res. 173 (2020), 115467, https://doi.org/10.1016/j.watres.2020.115467.
[13] L. Ma, J. Liang, Y. Liu, et al., Production of a bioflocculant from Enterobacter sp. P3 using brewery wastewater as substrate and its application in fracturing flowback water treatment, Environ. Sci. Pollut. Res. 27 (15) (2020) 18242–18253, https://doi.org/10.1007/s11356-020-08245-x.
[14] S.E.P. Administration, Comprehensive wastewater discharge standard: GB 8978–1996[S], Standards press of china, Beijing, 1996, pp. 274–275.
[15] A.V. Karim, A. Hassani, P. Eghbali, et al., Nanostructured modified layered double hydroxides (LDHs)-based catalysts: A review on synthesis, characterization, and applications in water remediation by advanced oxidation processes, Curr. Opin. Solid State Mater. Sci. 26 (1) (2022), 100965, https://doi.org/10.1016/j.cossms.2021.100965.
[16] Hassani A, Eghbali P, Mehdipour F, et al. Insights into the synergistic role of photocatalytic activation of peroxymonosulfate by UVA-LED irradiation over $CoFe_2O_4$-rGO nanocomposite towards effective Bisphenol A degradation: Performance, mineralization, and activation mechanism. Chemical Engineering Journal, 2022: 139556. 10.1016/ j.cej.2022.139556.
[17] M. Bahri, A. Mahdavi, A. Mirzaei, et al., Integrated oxidation process and biological treatment for highly concentrated petrochemical effluents: a review, Chemical Engineering and Processing-Process Intensification 125 (2018) 183–196, https://doi.org/10.1016/j.cep.2018.02.002.
[18] G. Boczkaj, A. Fernandes, Wastewater treatment by means of advanced oxidation processes at basic pH conditions: a review, Chem. Eng. J. 320 (2017) 608–633, https://doi.org/10.1016/j.cej.2017.03.084.
[19] Fedorov K, Dinesh K, Sun X, et al. Synergistic effects of hybrid advanced oxidation processes (AOPs) based on hydrodynamic cavitation phenomenon–a review. Chemical Engineering Journal, 2021: 134191. 10.1016/j.cej. 2021.134191.
[20] K. Fedorov, M. Plata-Gryl, J.A. Khan, et al., Ultrasound-assisted heterogeneous activation of persulfate and peroxymonosulfate by asphaltenes for the degradation of BTEX in water, J. Hazard. Mater. 397 (2020), 122804, https://doi.org/10.1016/j.jhazmat.2020.122804.
[21] K. Fedorov, X. Sun, G. Boczkaj, Combination of hydrodynamic cavitation and SR-AOPs for simultaneous degradation of BTEX in water, Chem. Eng. J. 417 (2021), 128081, https://doi.org/10.1016/j.cej.2020.128081.
[22] M. Pirsaheb, N. Moradi, Sonochemical degradation of pesticides in aqueous solution: investigation on the influence of operating parameters and degradation pathway–a systematic review, RSC Adv. 10 (13) (2020) 7396–7423, https://doi.org/10.1039/C9RA11025A.
[23] Y. Xiong, H.A. Zhou, G. Xiong, COD reduction treatment of flowback water from shale gas hydraulic fracturing based on oxidation with ozonation and ultrasound, Chemical progress (2022) 1–8.
[24] Alias N H, Jaafar J, Samitsu S, et al. Photocatalytic degradation of oilfield produced water using graphitic carbon nitride embedded in electrospun polyacrylonitrile nanofibers. Chemosphere, 2018, 204: 79-86. 10.1016/ j. chemosphere.2018.04.033.
[25] Campos V. Electrochemical treatment of Produced Water using Ti/Pt and BDD anode. International Journal of Electrochemical Science, 2018, 05(13): 7894-7906. 10.20964/2018.08.44.
[26] T.J. Mason, Industrial sonochemistry: potential and practicality, Ultrasonics 30 (3) (1992) 192–196, https://doi.org/10.1016/0041-624X(92)90072-T.
[27] A. Kotronarou, G. Mills, M.R. Hoffmann, Decomposition of parathion in aqueous solution by ultrasonic irradiation, Environ. Sci. Tech. 26 (7) (1992) 1460–1462, https://doi.org/10.1021/es00031a026.
[28] S. Koda, T. Kimura, T. Kondo, et al., A standard method to calibrate sonochemical efficiency of an individual reaction system, Ultrason. Sonochem. 10 (3) (2003) 149–156, https://doi.org/10.1016/S1350-4177(03)00084-1.
[29] P.R. Gogate, V.S. Sutkar, A.B. Pandit, Sonochemical reactors: important design and scale up considerations with a special emphasis on heterogeneous systems, Chem. Eng. J. 166 (3) (2011) 1066–1082, https://doi.org/10.1016/j.cej.2010.11.069.
[30] K. Suslick, D. Casadonte, S. Choe, et al., Heterogeneous Sonochemistry and Sonocatalysis, Science 247 (1990) 1439–1446.
[31] T.J. Mason, J.P. Lorimer, D.M. Bates, Quantifying Sonochemistry: Casting Some Light on a Black Art, Ultrasonics 30 (1) (1992) 40–42, https://doi.org/10.1016/0041-624X(92)90030-P.
[32] W. Li, V. Nanaboina, Q. Zhou, et al., Effects of Fenton treatment on the properties of effluent organic matter and their relationships with the degradation of pharmaceuticals and personal care products, Water Res. 46 (2) (2012) 403–412, https://doi.org/10.1016/j.watres.2011.11.002.
[33] J. Fick, H. Söderström, R.H. Lindberg, et al., Contamination of surface, ground, and drinking water from pharmaceutical production, Environ. Toxicol. Chem. 28 (12) (2009) 2522–2527, https://doi.org/10.1897/09-073.1.
[34] G. Cruz-González, K. González-Labrada, Y. Milián-Rodríguez, et al., Enhancement of paracetamol degradation by sono-Fenton process, Int J Chem Mater Environ Res 2 (2015) 37–45.
[35] P.R. Gogate, S. Mededovic-Thagard, D. McGuire, et al., Hybrid reactor based on combined cavitation and ozonation: from concept to practical reality, Ultrason. Sonochem. 21 (2) (2014) 590–598, https://doi.org/10.1016/j.ultsonch.2013.08.016.
[36] C.H. Weng, Y.T. Lin, C.K. Chang, et al., Decolourization of direct blue 15 by Fenton/ultrasonic process using a zero-valent iron aggregate catalyst, Ultrason. Sonochem. 20 (3) (2013) 970–977, https://doi.org/10.1016/j.ultsonch.2012.09.014.
[37] J.H. Sun, S.P. Sun, J.Y. Sun, et al., Degradation of azo dye Acid black 1 using low concentration iron of Fenton process facilitated by ultrasonic irradiation, Ultrason. Sonochem. 14 (6) (2007) 761–766, https://doi.org/10.1016/j.ultsonch.2006.12.010.
[38] B. Kakavandi, M. Ahmadi, Efficient treatment of saline recalcitrant petrochemical wastewater using heterogeneous UV-assisted sono-Fenton process, Ultrason. Sonochem. 56 (2019) 25–36, https://doi.org/10.1016/j.ultsonch.2019.03.005.
[39] X. Wu, J. Liu, J.J. Zhu, Sono-Fenton hybrid process on the inactivation of Microcystis aeruginosa: Extracellular and intracellular oxidation, Ultrason. Sonochem. 53 (2019) 68–76, https://doi.org/10.1016/j.ultsonch.2018.12.034.
[40] L. Xu, X. Zhang, J. Han, et al., Degradation of emerging contaminants by sono-Fenton process with in situ generated H2O2 and the improvement by P25-mediated visible light irradiation, J. Hazard. Mater. 391 (2020), 122229, https://doi.org/10.1016/j.jhazmat.2020.122229.
[41] J.M. Philip, C.M. Koshy, U.K. Aravind, et al., Sonochemical degradation of DEET in aqueous medium: Complex by-products from synergistic effect of sono-Fenton–New insights from a HRMS study, J. Environ. Chem. Eng. 10 (3) (2022), 107509, https://doi.org/10.1016/j.jece.2022.107509.
[42] R. Huang, Z. Fang, X. Yan, et al., Heterogeneous sono-Fenton catalytic degradation of bisphenol A by Fe_3O_4 magnetic nanoparticles under neutral condition, Chem. Eng. J. 197 (2012) 242–249, https://doi.org/10.1016/j.cej.2012.05.035.
[43] F.Z. Huang, X. Fang, et al., Ultrasonic Fenton-like catalytic degradation of bisphenol A by ferroferric oxide (Fe_3O_4) nanoparticles prepared from steel pickling waste liquor, J. Colloid Interface Sci. 436 (2014) 258–266, https://doi.org/10.1016/j.jcis.2014.08.035.
[44] T.J. Al-Musawi, H. Kamani, E. Bazrafshan, et al., Optimization the effects of physicochemical parameters on the degradation of cephalexin in Sono-Fenton

reactor by using box-Behnken response surface methodology, Catal. Lett. 149 (5) (2019) 1186–1196, https://doi.org/10.1007/s10562-019-02713-x.
[45] K. González Labrada, D.R. Alcorta Cuello, I. Saborit Sánchez, et al., Optimization of ciprofloxacin degradation in wastewater by homogeneous Sono-Fenton process at high frequency, J. Environ. Sci. Health A 53 (13) (2018) 1139–1148, https://doi.org/10.1080/10934529.2018.1530177.
[46] A. Khataee, P. Gholami, B. Vahid, et al., Heterogeneous sono-Fenton process using pyrite nanorods prepared by non-thermal plasma for degradation of an anthraquinone dye, Ultrason. Sonochem. 32 (2016) 357–370, https://doi.org/10.1016/j.ultsonch.2016.04.002.
[47] Prajapat A L, Gogate P R. Depolymerization of guar gum solution using different approaches based on ultrasound and microwave irradiations. Chemical Engineering and Processing: Process Intensification, 2015, 88: 1-9. https://doi.org/10.1016/j.cep.2014.11.018.
[48] Y.M. Lou, Development and Application of Low-Damage Heat-Resisting Fracturing Fluids, Northeast Petroleum University (2013).
[49] P.R. Gogate, I.Z. Shirgaonkar, M. Sivakumar, et al., Cavitation reactors: efficiency assessment using a model reaction, AIChE J 47 (11) (2001) 2526–2538, https://doi.org/10.1002/aic.690471115.
[50] J. Li, S. Guo, X. Li, Degradation kinetics of polystyrene and EPDM melts under ultrasonic irradiation, Polym. Degrad. Stab. 89 (1) (2005) 6–14, https://doi.org/10.1016/j.polymdegradstab.2004.12.017.
[51] National General Administration of Environmental Protection, Water quality-determination of the chemical oxygen demand-fast digestion-spectrophotometric method: HJ/T 399–2007[S], China Environmental Science Press, Beijing, 2007.
[52] X.H. Deng, H.T. Zhang, G.M. Cao, et al., Study on the effect of hydrogen peroxide on determination of chemical oxygen demand, Shanghai Chemical industry 36 (04) (2008) 11–13.
[53] Li H. Study on Treatment of PAHs Dye Wastewater by Fenton Advanced Oxidation Process. Chongqing University, 2007.
[54] Y.C.W. Fenton, and Electro-Fenton Technology for Treatment of Heterocyclic Organic Wastewater with Modified Catalyst, Dalian University of Technology, 2012.
[55] D.W. O'Sullivan, M. Tyree, The kinetics of complex formation between Ti (IV) and hydrogen peroxide, Int. J. Chem. Kinet. 39 (8) (2007) 457–461, https://doi.org/10.1002/kin.20259.
[56] L.J. Xu, W. Chu, N. Graham, Degradation of di-n-butyl phthalate by a homogeneous sono–photo–Fenton process with in situ generated hydrogen peroxide, Chem. Eng. J. 240 (2014) 541–547, https://doi.org/10.1016/j.cej.2013.10.087.
[57] Acisli, Ozkan, Khataee, et al. Combination of ultrasonic and Fenton processes in the presence of magnetite nanostructures prepared by high energy planetary ball mill. Ultrasonics Sonochemistry, 2017, 34: 754-762. 10.1016/j.ultsonch.2016.07.011.
[58] National General Administration of Environmental Protection, Standard for pollution control of sewage Marine treatment engineering: GB 18486–2016[S], China Environmental Science Press, Beijing, 2016.
[59] H.C. Yap, Y.L. Pang, S. Lim, et al., A comprehensive review on state-of-the-art photo-, sono-, and sonophotocatalytic treatments to degrade emerging contaminants, Int. J. Environ. Sci. Technol. 16 (2019) 601–628, https://doi.org/10.1007/s13762-018-1961-y.
[60] A M S, B R F, C G J P. Synergistic effects of combining ultrasound with the Fenton process in the degradation of Reactive Blue 19. Ultrasonics Sonochemistry, 2014, 21(3): 1206-1212. 10.1016/j.ultsonch.2013.12.016.
[61] N.N. Wang, Q. Zhao, Q.Y. Li, et al., Degradation of polyacrylamide in an ultrasonic-Fenton-like process using an acid-modified coal fly ash catalyst, Powder Technol. 369 (2020) 270–278, https://doi.org/10.1016/j.powtec.2020.05.052.
[62] U. Menon, N. Suresh, G. George, et al., A study on combined effect of Fenton and Free Nitrous Acid treatment on sludge dewaterability with ultrasonic assistance: Preliminary investigation on improved calorific value, Chem. Eng. J. 382 (2020), 123035, https://doi.org/10.1016/j.cej.2019.123035.
[63] N. Jaafarzadeh, A. Takdastan, S. Jorfi, et al., The performance study on ultrasonic/Fe3O4/H2O2 for degradation of azo dye and real textile wastewater treatment, J. Mol. Liq. 256 (2018) 462–470, https://doi.org/10.1016/j.molliq.2018.02.047.
[64] M. Verma, A.K. Haritash, Degradation of amoxicillin by Fenton and Fenton-integrated hybrid oxidation processes, J. Environ. Chem. Eng. 7 (1) (2019), 102886, https://doi.org/10.1016/j.jece.2019.102886.
[65] S. Merouani, O. Hamdaoui, F. Saoudi, et al., Sonochemical degradation of Rhodamine B in aqueous phase: Effects of additives, Chem. Eng. J. 158 (3) (2010) 550–557, https://doi.org/10.1016/j.cej.2010.01.048.
[66] M.S. Lucas, J.A. Peres, Removal of COD from olive mill wastewater by Fenton's reagent: kinetic study, J. Hazard. Mater. 168 (2–3) (2009) 1253–1259, https://doi.org/10.1016/j.jhazmat.2009.03.002.
[67] L. Zhang, F. Su, N. Wang, et al., Biodegradability enhancement of hydrolyzed polyacrylamide wastewater by a combined Fenton-SBR treatment process, Bioresour. Technol. 278 (2019) 99–107, https://doi.org/10.1016/j.biortech.2019.01.074.
[68] D. Panda, S. Manickam, Heterogeneous Sono-Fenton treatment of decabromodiphenyl ether (BDE-209): Debromination mechanism and transformation pathways, Sep. Purif. Technol. 209 (2019) 914–920, https://doi.org/10.1016/j.seppur.2018.06.069.
[69] A.L. Prajapat, P. Das, P.R. Gogate, A novel approach for intensification of enzymatic depolymerization of carboxymethyl cellulose using ultrasonic and ultraviolet irradiations, Chem. Eng. J. 20 (1) (2016) 391–399, https://doi.org/10.1016/j.cej.2016.01.074.
[70] G.Q. Nie, Y.G. Wu, X. Li, et al., Research progress on main influencing factors of ultrasonic technology in water treatment, Technol. Water Treat. 34 (3) (2008) 11–14.
[71] W. Wang, W. Chen, M. Zou, et al., Applications of power ultrasound in oriented modification and degradation of pectin: A review, J. Food Eng. 234 (2018) 98–107, https://doi.org/10.1016/j.jfoodeng.2018.04.016.
[72] A.L. Prajapat, P.B. Subhedar, P.R. Gogate, Ultrasound assisted enzymatic depolymerization of aqueous guar gum solution, Ultrason. Sonochem. 29 (2016) 84–92.
[73] E. Basturk, M. Karatas, Advanced oxidation of Reactive Blue 181 solution: A comparison between Fenton and Sono-Fenton Process, Ultrason. Sonochem. 21 (5) (2014) 1881–1885, https://doi.org/10.1016/j.ultsonch.2014.03.026.
[74] E. Psillakis, G. Goula, N. Kalogerakis, et al., Degradation of polycyclic aromatic hydrocarbons in aqueous solutions by ultrasonic irradiation, J. Hazard. Mater. 108 (1–2) (2004) 95–102, https://doi.org/10.1016/j.jhazmat.2004.01.004.
[75] G. Nie, K. Hu, W. Ren, et al., Mechanical agitation accelerated ultrasonication for wastewater treatment: Sustainable production of hydroxyl radicals, Water Res. 198 (2021), 117124, https://doi.org/10.1016/j.watres.2021.117124.
[76] Z. Zhi, J. Li, J. Chen, et al., Preparation of low molecular weight heparin using an ultrasound-assisted Fenton-system, Ultrason. Sonochem. 52 (2019) 184–192, https://doi.org/10.1016/j.ultsonch.2018.11.016.
[77] H. Ghodbane, O. Hamdaoui, Intensification of sonochemical decolorization of anthraquinonic dye Acid Blue 25 using carbon tetrachloride, Ultrason. Sonochem. 16 (4) (2009) 455–461, https://doi.org/10.1016/j.ultsonch.2008.12.005.
[78] Y. Tang, H. Ren, P. Yang, et al., Treatment of fracturing fluid waste by Fenton reaction using transition metal complexes catalyzes oxidation of hydroxypropyl guar gum at high pH, Environ. Chem. Lett. 17 (1) (2019) 559–564, https://doi.org/10.1007/s10311-018-0805-9.
[79] K.H. Chan, W. Chu, Modeling the reaction kinetics of Fenton's process on the removal of atrazine, Chemosphere 51 (4) (2003) 305–311, https://doi.org/10.1016/S0045-6535(02)00812-3.
[80] A. Hassani, P. Eghbali, A. Ekicibil, et al., Monodisperse cobalt ferrite nanoparticles assembled on mesoporous graphitic carbon nitride (CoFe2O4/mpg-C3N4): a magnetically recoverable nanocomposite for the photocatalytic degradation of organic dyes, J. Magn. Magn. Mater. 456 (2018) 400–412, https://doi.org/10.1016/j.jmmm.2018.02.067.
[81] X. Luo, H. Gong, Z. He, et al., Recent advances in applications of power ultrasound for petroleum industry, Ultrason. Sonochem. 70 (2021), 105337, https://doi.org/10.1016/j.ultsonch.2020.105337.